International Journal of Pharmaceutics 534 (2017) 220–228

Contents lists available at ScienceDirect

International Journal of Pharmaceutics

journal homepage: www.elsevier.com/locate/ijpharm

Spontaneous nano-emulsification: Process optimization and modeling for the prediction of the nanoemulsion's size and polydispersity

G. Lefebvre*, J. Riou, G. Bastiat, E. Roger, K. Frombach, J-C. Gimel, P. Saulnier, B. Calvignac

Micro & Nanomédecines Translationelles-MINT, UNIV Angers, INSERM U1066, CNRS UMR 6021, UBL Université Bretagne Loire, Angers F-49933, France

ARTICLE INFO

Keywords:
Nanoemulsion
Spontaneous emulsification
Low-energy methods
Mixture experiments

ABSTRACT

The aim of the present study was to optimize the size and polydispersity of a lipid nanoemulsion as a function of the oil (Labrafac® WL1349), surfactant (Kolliphor® HS 15) and cosurfactant (Span® 80) phase composition and temperature. The nanoemulsions were prepared using a low-energy self-emulsification method. The Z-average diameter and the polydispersity index (PDI) were modeled with mixture experiments. Nanoemulsions from 20 nm to 120 nm with PDI < 0.2 were obtained at the three different tested temperatures (30 °C, 50 °C and 90 °C). The nanoemulsion size was able to be controlled with the oil, surfactant and cosurfactant concentrations. Interestingly, the smallest PDIs were obtained at 30 °C, and the cosurfactant concentration was able to be adjusted to optimize the formulation and to obtain nanoemulsions in the 20–120 nm range with a PDI smaller than 0.14. These nanoemulsions have shown a good stability at 4 °C in storage conditions and at 37 °C in diluted conditions.

1. Introduction

Lipid core nanoformulations (LNFs) can include various types of structure, such as lipid nano-emulsions (LNEs), solid lipid nanoparticles (SLNs), nanostructured lipid carriers or lipid nanocapsules (LNCs) (Matougui et al., 2016). This study is dedicated to the LNEs. LNEs are of a great importance because of the wide range of applications such as drug delivery (Hörmann and Zimmer, 2016; Khani et al., 2016; Mishra et al., 2015), cosmetics (Montenegro et al., 2016; Yukuyama et al., 2016) and food (Goindi et al., 2016; Komaiko and McClements, 2016; McClements, 2011). Despite their-out-of equilibrium state, LNEs are highly kinetically stable formulations. The most common techniques to formulate LNEs are the so-called high-energy methods. These techniques are mainly ultrasound generators and/or high-pressure homogenizers (Calligaris et al., 2016), supplying enough energy to increase water/oil interfacial area causing the generation of submicronic droplets. These techniques are quite straightforward to implement but they are cost-inefficient and can be unsuitable for thermo- and mechano-sensitive molecules, such as proteins or peptides (Kuhn and Cunha, 2012; Pchelintsev et al., 2016). Therefore, in an ecological approach and in using softer conditions, the last decades have seen the apparition of low-energy methods to produce the LNEs. These methods include phase inversion temperature (PIT) (Anton et al., 2007; Izquierdo et al., 2004; Shinoda and Saito, 1968, 1969), phase inversion composition (PIC) (Forgiarini et al., 2000, 2001) or spontaneous (Bouchemal et al., 2004; Trotta et al., 2001) methods. Seeing the numerous reviews in the last twelve years dedicated to the production of LNEs as final objects (Gutiérrez et al., 2008; Komaiko and McClements, 2016; Singh et al., 2017; Solans et al., 2005; Solans and Solé, 2012) or as templates (Anton et al., 2008; Blin et al., 2016), it is obvious that the different methods of formulation, particularly the low-energy ones, have been deeply investigated.

With this development of techniques to produce nanoformulation systems, some authors focused on the clarification of the differences between nanoemulsions and microemulsions (Anton and Vandamme, 2011; McClements, 2012). These two systems can present similar structures, e.g. nanodroplets of oil in water in LNEs and micelles swollen with oil in microemulsions, but their stability remains very different. Microemulsions are thermodynamically stable, under certain conditions only, with equilibrated interfaces while LNEs are thermodynamically unstable, with more or less dynamically arrested interfaces that provide a kinetic stability to nanodroplets. This stability difference is explained by a difference between the free energy ΔG of the colloidal dispersions (nano- or microemulsions) and the free energy of the separated phases (organic and aqueous) from which they are prepared. Microemulsions have a lower free energy than the separated phases, whereas LNEs have a higher free energy. In addition to this stability difference, the way of formulation, i.e. the order in which the different compounds are mixed, is important. Unlike the microemulsions, LNEs obtained by a self-emulsifying method are only formed if surfactants are

* Corresponding author at: Laboratoire MINT UMR INSERM U1066/CNRS 6021, IBS-CHU ANGERS, 4 rue Larrey, 49933 ANGERS CEDEX 9, France.
E-mail address: guillaume.lefebvre@univ-angers.fr (G. Lefebvre).

http://dx.doi.org/10.1016/j.ijpharm.2017.10.017
Received 26 July 2017; Received in revised form 3 October 2017; Accepted 9 October 2017
Available online 14 October 2017
0378-5173/

first mixed with the oily phase, before mixing it with the aqueous phase. Finally, these two systems differ in their behavior towards temperature and concentration variations. The nano-structures of microemulsions can be strongly affected (morphology and size) or even broken up by a modification of the temperature or a dilution, while nanodroplets of a nanoemulsion can remain stable in such stressing conditions. In this way, as some routes of administration can create these conditions, e.g. parenteral route, the LNEs arouse interest as stable drug delivery systems even after some dilution or temperature modifications (Hörmann and Zimmer, 2016).

The mechanisms implied in the different low-energy methods are discussed to be unique (Anton and Vandamme, 2009), but these methods are still distinguished in the literature. One classification is based on whether or not a spontaneous inversion of the surfactant curvature takes place during the emulsification process; this is the case in the PIT and PIC methods. In the case where a LNE formation is caused by the rapid diffusion of surfactant(s) from the oil phase to the oil/water interface, the method is referred to as "spontaneous" or "self-emulsifying". In pharmaceutical development, these nanoemulsions can be spontaneously formed in the gastrointestinal tract environment. In this case, they are called Self-Nano-Emulsifying Drug Delivery Systems (SNEDDS) (Date et al., 2010). Furthermore, the spontaneous LNEs can be formulated *ex-vivo*, as in this study. In the drug delivery field, these last formulated LNEs can be administered by different routes such as topical, oral, intravenous, intranasal, pulmonary, or ocular (Singh et al., 2017). They are promising candidates to improve therapeutic effects (Bouchaala et al., 2016) and they already showed oral bioavailability improvements (Zhao et al., 2013).

However, before incorporating a drug into a self-nano-emulsifying system, it is of a great interest to increase the knowledge of the effects of some factors on LNE formulation. Indeed, drugs that can be potentially encapsulated in a lipidic nano-carrier may be affected by the formulation processes (Anton et al., 2008). For instance, the incorporation of a thermo-sensitive drug can involve an adjustment of the formulation to reduce the process temperature. From an ecological point of view, a temperature decrease helps to develop eco-friendly processes and makes them easier to implement, which is another important reason to be able to adjust formulation. On one hand, the new formulation must provide similar required nanodroplets, i.e. same diameter and polydispersity index. On the other hand, the new formulation must stay stable in biological conditions. Here, the LNE formulation process was based on spontaneous emulsification without using additional solvent, which has been previously described by Anton and Vandamme (Anton and Vandamme, 2009). Previous studies theoretically discussed the importance of components' properties used for the fabrication of self-nano-emulsifying systems, e.g. the oily phase composition or the surfactant's hydrophilic-lipophilic balance (HLB) (Bouchemal et al., 2004; Date et al., 2010). Moreover, the spontaneous nanoemulsification method has already been studied using oil/surfactant/cosurfactant ternary phase diagrams, but more particularly this method has been studied to identify the self-nano-emulsifying region (Date and Nagarsenker, 2007; Dixit and Nagarsenker, 2008; Shen et al., 2016; Yoo et al., 2010). Finally, only a few studies have investigated the effect of temperature on LNE properties (An et al., 2014; Komaiko and McClements, 2015a; Saberi et al., 2013). The present work has investigated the effect of temperature and composition on LNE size and polydispersity and the stability of a system composed of nonionic surfactant(s) (Kolliphor® HS 15 and Span® 80), medium chain triglycerides (Labrafac® WL1349) and water, which are Generally Recognized As Safe (GRAS) ingredients. The originality was the use of mixture experiments to design a model for the prediction of the LNE criteria (size and polydispersity) as a function of the oily phase composition. Furthermore, the model has been systematically analyzed at three different temperatures (30, 50 and 90 °C) for the organic phase, added water remaining at room temperature.

2. Materials and methods

2.1. Materials

Nonionic surfactant Kolliphor® HS 15 (mixture of free PEG 660 and *PEG 660*-12-hydroxystearate, HLB ~ 14–16) and cosurfactant Span® 80 (sorbitan monoleate, HLB ~ 4–5) were respectively provided by BASF (Ludwigshafen, Germany) and Sigma-Aldrich Co. (Saint Quentin Fallavier, France). The oily phase, i.e. Labrafac® WL1349 (medium-chain triglycerides MCT), was purchased from Gattefossé (Saint-Priest, France). These three ingredients will be respectively referred to as Kolliphor, Span and Labrafac in this paper. Ultrapure water was obtained from a MilliQ filtration system (Millipore, Saint-Quentin-en-Yvelines, France).

2.2. LNE formation by spontaneous emulsification

LNE formation was carried out using spontaneous nano-emulsification method. Briefly, the organic phase (oil, surfactant and cosurfactant) was heated at a minimum of 30 °C to solubilize the Kolliphor (solid at room temperature) in the oil. When this mixture reached the desired temperature, the magnetic stirring was increased from 850 rpm to 1200 rpm and water at room temperature (20 °C–25 °C) was poured in, all at one time, to shape the nanoemulsion. After the addition of water, the stirring was maintained for 5 min at room temperature.

Different LNEs were prepared with different surfactants-to-oil mass ratios (SOR, Eq. (1)) and different cosurfactant-to-surfactant mass ratios, i.e. Span-to-Kolliphor mass ratios (SpKR, Eq. (2)). Only one surfactant and oil-to-water mass ratio (SOWR, Eq. (3)) of 0.047 has been tested.

$$\mathrm{SOR} = \frac{\mathrm{mass}_{\mathrm{Kolliphor}} + \mathrm{mass}_{\mathrm{Span}}}{\mathrm{mass}_{\mathrm{Labrafac}}} \quad (1)$$

$$\mathrm{SpKR} = \frac{\mathrm{mass}_{\mathrm{Span}}}{\mathrm{mass}_{\mathrm{Kolliphor}}} \quad (2)$$

$$\mathrm{SOWR} = \frac{\mathrm{mass}_{\mathrm{Kolliphor}} + \mathrm{mass}_{\mathrm{Span}} + \mathrm{mass}_{\mathrm{Labrafac}}}{\mathrm{mass}_{\mathrm{water}}} \quad (3)$$

A first screening was carried out heating the organic phase at 90 °C and pouring water at 4 °C. For the designed mixture experiments, three temperatures were tested for the organic phase: 30 °C, 50 °C and 90 °C (see 2.5). Moreover, a second screening (data not shown), with some various compositions, has been carried out with a water temperature addition at room temperature. The obtained LNEs were formulated in the same 20–120 nm range. Finally, the water temperature addition was fixed at room temperature (20–25 °C) for the mixture experiments.

2.3. Viscosity measurements

The absolute viscosity μ (newtonian flow profile determined at shear rates from 1 to 100 s^{-1}) of Kolliphor + Labrafac mixtures (for different SORs) was measured from 30 °C to 90 °C, using a Kinexus® rheometer (Malvern Instruments S.A., United Kingdom), with a parallel plate geometry (diameter: 20 mm, gap: 700 µm).

2.4. LNE size measurements

The LNE size measurements were carried out by dynamic light scattering using a Malvern Nano-S instrument (Malvern Instrument Ltd., Worcestershire, UK). The helium–neon laser, 4 mW, operates at 633 nm, with a scattering angle fixed at 173°. The mean droplets diameter d (obtained from the Z-average diffusion coefficient) and the polydispersity index (PDI) were calculated from the auto-correlation

function of the electric field, fitted using the cumulant analysis (Berne and Pecora, 2000).

2.5. Mixture experiments

Three components of interest were used: Kolliphor, Labrafac and Span with their respective weight fraction: $0.25 < L < 0.55$, $0.35 < K < 0.65$ and $0 < Sp < 0.20$. A pseudo-ternary diagram was realized on the feasibility domain composed of 25 separated experiments. Based on an incomplete quadratic model, the results of experiments and the factors of interest allowed for a model with two different outcomes Y, i.e. the LNE droplets average diameter d and the polydispersity index PDI. The choice of interactions was based on manual stepwise variable selection.

With each separate experiment identified as the i parameter, with $1 \leq i \leq 25$, and its repetition as the j parameter, $1 \leq j \leq 4$, the model was defined as:

$$Y_{ij} = \beta_1 K_{ij}^2 + \beta_2 K_{ij} + \beta_3 L_{ij}^2 + \beta_4 L_{ij} + \beta_5 Sp_{ij}^2 + \beta_6 Sp_{ij} + \beta_7 (K_{ij} Sp_{ij}) + \varepsilon_{ij}, \quad \varepsilon_{ij} \overset{i.i.d}{\sim} N(0, \sigma_Y^2) \tag{4}$$

Where β_k were the model coefficients, obtained by maximum likelihood estimation (MLE), with $1 \leq k \leq 7$, and ε_{ij} the residuals, independent and identically distributed (i.i.d) following a normal distribution with mean zero and variance σ_Y^2.

The model performances were measured according to the adjusted coefficient of determination (R^2) and to the lack of fit Fisher test. Mixture experiments design and experimental results analysis were done with mixexp (Lawson and Willden, 2016) package from R software (R Development Core Team, 2014). The central point of the ternary diagram was carried out at least four times, for each temperature, to estimate the intra-experiment dispersion.

2.6. LNE stability

Since these LNEs could be used as drug delivery systems, their stability was investigated both at 4 °C (without dilution to mimic storage conditions) and at 37 °C (with dilution to mimic operating conditions for future *in vitro* and *in vivo* studies). Just after their formulation, a volume of 10 µL was removed from the stock LNEs and put in cuvettes (DTS0012, Malvern Instrument Ltd., Worcestershire, UK) in order to create a 1/400 dilution by addition of 3990 µL of ultrapure water. These cuvettes were used for LNE size measurements at t_0 at 25 °C.

For 4 °C stability, the stock suspensions were stored at 4 °C and diluted at regular intervals with a 1/7 dilution for LNE size measurements during one month.

For 37 °C stability, the cuvettes containing the 1/400 diluted solutions were stored at 37 °C and they were used as they were for the LNE size measurements at regular intervals during two weeks.

3. Results and discussions

3.1. Screening of formulations

In order to initialize the mixture experiments, a preliminary screening was carried out to define the Design Space (DS) of the model with the study of the Factor Space (organic phase composition, i.e. SOR and SpKR) and the Response Space (Z-average diameter and PDI). The Factor Space design was based on the composition of LNCs (Heurtault et al., 2003) and from the laboratory expertise (Béduneau et al., 2008; Heurtault et al., 2001; Huynh et al., 2009; Roger et al., 2009). Consequently, around thirty LNEs were formulated with various SOR between 0.8 and 2.6 and different SpKR between 0 and 0.4. Besides, for a SpKR = 0 and with a SOWR = 0.047, the LNE size obtained for different SOR is similar to LNE size obtained by Anton et al. with a SOWR = 0.43 (Anton and Vandamme, 2009). Then, considering that the amount of added water had no significant effect on the LNE size, only one SOWR of 0.047 was chosen to be tested. The targeted Response Space is based on nanomedicine applications, i.e. 20–120 nm. Results of this screening are introduced in Fig. 1.

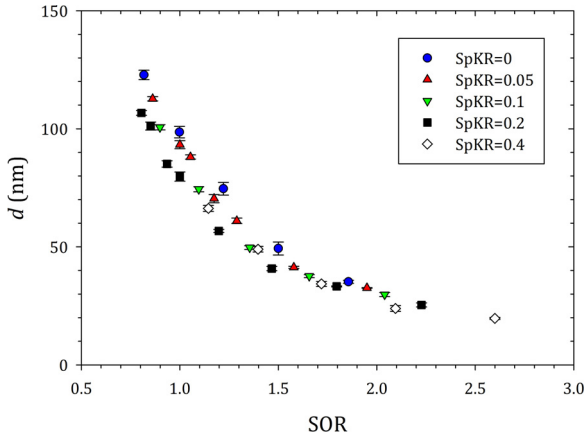

Fig. 1. Evolution of the Z-average diameter of LNEs as a function of the SOR for various SpKR as indicated in the figure (n = 3; mean ± SD).

With all the tested compositions, the LNEs were in the required size range from 20 nm to 120 nm. As expected and already observed (Davidov-Pardo and McClements, 2015; Saberi et al., 2013), the size of the LNEs decreased with the increase of the SOR. More precisely, whatever the SpKR, a strong decrease of the nanodroplets average diameter was noted for a SOR increasing from 0.8 to 1.5, the diameter decreasing from around 110–120 nm to around 40–50 nm. Above a SOR of 1.5, the effect was less important and the nanodroplets diameter stayed between 20 nm and 40 nm. Furthermore, the effect of the SpKR for a unique SOR was also noticed. For instance, for a SOR of 1, the LNE size decreased from 100 nm (SpKR = 0) to 80 nm (SpKR = 0.2). For one given SOR, an increase of SpKR from zero to 0.2 induced a decrease of the surfactant mixture HLB from around 15 (pure Kolliphor), to 12.9. This result was not necessarily consistent with other studies in which a decrease of the HLB was correlated with an increase of the LNE size (Bouchemal et al., 2004; Komaiko and McClements, 2015b). However, our results could be in line with the interpretation of Anton et al. (Anton and Vandamme, 2009) who considered that the determining factor governing spontaneous LNE formation may be the affinity of the surfactants for the hydrophobic phase. In other words, the HLB of the surfactant needs to be sufficiently low to show a good solubility in the oil and sufficiently high to ensure a quick and complete diffusion from the oil phase to the oil/water interface. Therefore, for a specific couple of organic and aqueous phases, there may exist a critical HLB for which the smallest droplets diameter is achieved. Various studies already suggested this critical HLB value as the key factor for the formulation of emulsions with a minimal droplets diameter (Lin et al., 1975; Pouton, 1997; Sagitani, 1981). An optimal HLB value between 10 and 11.5 has already been found with PIT formulated LNEs using paraffin oil and mixtures of Span® 80 and Tween® 80 (Liu et al., 2006). Another optimal HLB of 13.4 was obtained with Tween® 80 and Span® 20 as surfactants mixture for the formulation of spontaneous LNEs (An et al., 2014). However, it is now well known that the HLB concept is not as trivial. Indeed, using two surfactants with close HLB but different structures, i.e. Tween® 80 (HLB = 15) and Cremophor® RH40 (HLB ~ 14–16), Zeng and Zhang (Zeng and Zhang, 2016) formulated nanoemulsions with significantly different diameters, respectively 103.1 ± 1.29 and 62.28 ± 0.32 nm. It is important to keep in mind that the HLB does not take into account some critical parameters such as the environment (type of aqueous and organic phases), the temperature or the molecular geometry (Dai et al., 1997; Israelachvili, 2011; Saberi et al., 2013).

Concerning the PDI, Fig. 2 shows that for a SpKR between zero and

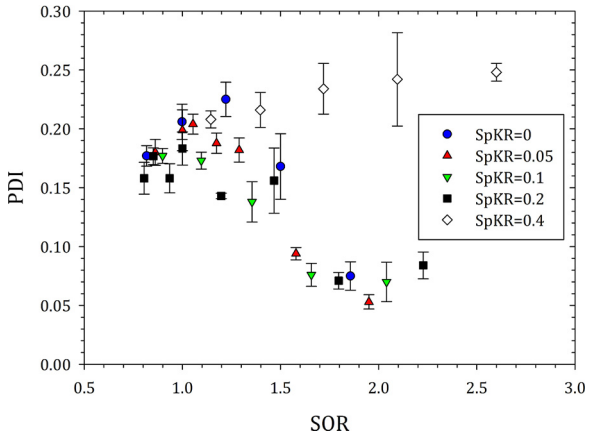

Fig. 2. Evolution of the PDI as a function of the SOR for various SpKR as indicated in the figure. (n = 3; mean ± SD).

0.2 an increase of SOR induced a decrease of the PDI, particularly for a SOR above 1.5. However, no significant effect of the SpKR was observed within that range. On the contrary, for the formulations with a SpKR of 0.4 the PDI showed an increase with a SOR increase. For this highest concentration of lipophilic Span, the formulation of the LNE seemed to be affected leading to less monodisperse LNEs. Besides, it is supposed that this Span concentration could strongly affect the diffusion of the surfactants mixture from the oil to the oil-water interface when water is added. Thus, it could have induced oil nanodroplets with higher diameter dispersion.

These screening results allowed a choice of the Labrafac, Kolliphor and Span concentrations intervals used for the mixture experiments analysis.

3.2. Design and analysis of mixture experiments

3.2.1. Mixture experiments design

The Design Space (weight fractions) was the following: 0.25 < Labrafac < 0.55, 0.35 < Kolliphor < 0.65 and 0 < Span < 0.20. The fourth component, i.e. water, was fixed. Thus, the Design Space can be illustrated on a ternary diagram (Fig. 3). The corresponding values of each point are given in Table S1 of the Supplementary material.

The three tested temperatures were chosen with respect to the clear points of the organic phase, visually observed during screening experiments. Usually, a cloud point of a nonionic surfactant is the temperature above which an aqueous solution of this surfactant becomes turbid because a rich phase of swollen micelles separates. Here, the nonionic surfactant (and eventually cosurfactant) was firstly mixed with the oil and the term “clear point” (CP) was used to characterize the temperature at which the organic phase goes from a turbid to a clear state as it is heated. As a function of SOR and SpKR, this CP was found to occur in a temperature range from 52 °C to 85 °C. Therefore, we decided to study the formulation of LNEs at three temperatures for the organic phase (surfactant + cosurfactant + oil):

- The “classical” temperature of 90 °C (Anton and Vandamme, 2009) which was above the CP for all compositions,
- 50 °C which was just below the lowest CP,
- 30 °C which was far below the lowest CP.

From an ecological point of view and in order to formulate thermosensitive active molecules, it is of a great interest to be able to prepare spontaneous LNEs at low temperature.

For the aqueous phase, only the room temperature (20 °C–25 °C) was investigated.

3.2.2. Mixture experiments analysis and modeling

Mixture experiments were aimed to model droplets’ average diameter and PDI with the mixture compositions for three temperatures (30 °C, 50 °C and 90 °C) of the organic phase. Considering the values obtained for the adjusted coefficient of determination (R^2) and for the lack of fit (Table 1), the chosen incomplete linear-quadractic models could be considered as reliable and presenting a good prediction within all the Design Space. Furthermore, as described in Section 2.4, the choice of the interaction term (K.Sp), based on statistical criteria, completely matched with physico-chemistry knowledge.

The results of mixture experiments were illustrated using pseudo-ternary diagrams (Fig. 4). The values obtained for the β coefficients (Eq. (4)) are given in the Supplementary material (Table S2).

3.2.2.1. Composition effect. To understand the influence of each organic phase component on the LNE diameter, effect plots were drawn (Fig. 5). In this plot, the centroid is the centre of gravity of the Design Space, i.e. sample n° 7 in the pseudo-ternary diagram (Fig. 3). It corresponds to the following weight proportions for the three organic phase components: 40% of Labrafac, 50% of Kolliphor and 10% of Span. The centroid was selected as a reference mixture and imaginary lines were drawn to predict the effect of pure component variation on the predicted response, i.e. the LNE size in Fig. 5. The deviation from centroid corresponds to a weight proportion variation for a pure component, while keeping constant the ratio of the two others (Cox, 1971).

For the three tested temperatures, the components had the same impact on the LNE size. The Labrafac concentration had the major effect on the diameter. When it increased, the LNE size strongly increased. As the effect of each component is plotted while keeping constant the ratio of the two others, it is obvious that for the same quantity of surfactants, the presence of more Labrafac induced the presence of more oil inside the droplets and therefore the formulation of larger LNEs. For the Kolliphor and Span, the effect on the LNE size

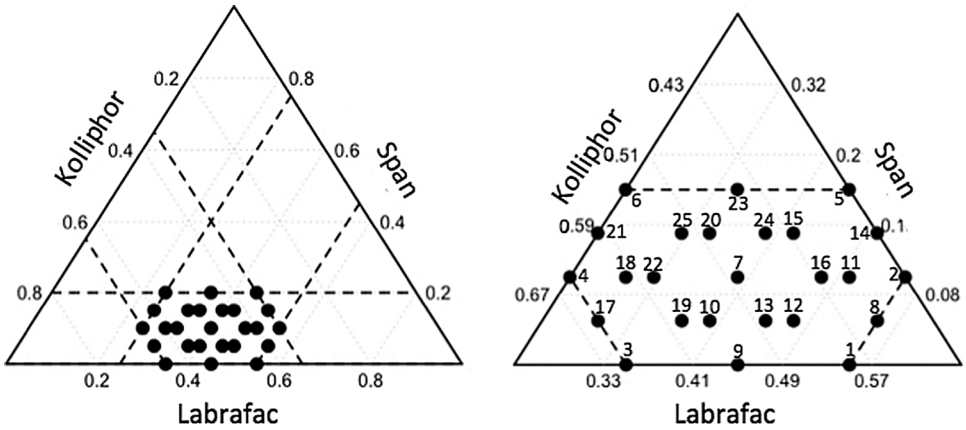

Fig. 3. Ternary (left) and pseudoternary (right) diagrams for the mixture experiments.

Table 1
Values of the adjusted coefficient of determination and of the lack of fit obtained for the incomplete linear-quadratic models.

	R^2		Lack of fit Fischer Test	
	d	PDI	*d* (*p*-value)	PDI (*p*-value)
30 °C	0.9941	0.9300	0.8452	0.3938
50 °C	0.9964	0.8890	0.7095	0.8859
90 °C	0.9950	0.8982	0.9716	0.9846

could be considered as analogous in view of their two parallel plots. The surfactant concentration was considered as an essential factor to control when using the spontaneous emulsification method. Indeed, it was important to use enough surfactant to form small droplets, but not too much as to avoid excess surfactant amount with large clump formation (Komaiko and McClements, 2016). In the tested concentration ranges ($0.8 < SOR < 3$ and $0 < SpKR < 0.57$), the increase of surfactant and cosurfactant concentrations led to a decrease of the LNE size.

3.2.2.2. Temperature effect. Firstly, as shown in Fig. 4., LNEs were able to be formulated at the three tested temperatures. This means that even at temperatures below the CP (30 °C and 50 °C), LNEs were able to be obtained. It leads to question the meaning of this CP. A first hypothesis it that the CP could be related to the dissolution point of the surfactant (s) in the oil. However, it is hard to believe that LNEs could even be formed below that point and show the same sizes as above the CP. Another hypothesis could originate from the presence of a non-negligible amount of free PEG chains in the Kolliphor (around 30% w/w of the total Kolliphor mass (Zhang et al., 2016)). Indeed, those PEG molecules are completely insoluble in aliphatic chains of Labrafac. The hypothesis is that above the CP, those chains could "hide" in nanostructured domains formed by the surfactants in the oil, especially by the *PEG 660*-12-hydroxystearate, the main coumpound of Kolliphor.

For all formulation temperatures, the obtained size ranges were similar and went from 30 nm to 120 nm. No significant differences in size were noticed between the three different temperatures. With another system ((vitamin E acetate + MCT)/Tween® 80/water), Saberi et al. (Saberi et al., 2013) observed a decrease of the LNE size from 107 to 89 nm for an organic phase temperature increase from 25 °C to 90 °C with a SOR = 0.5, keeping added water at room temperature. For a SOR = 1, this effect was less important and the size decreased from 55 to 48 nm. Komaiko et al. (Komaiko and McClements, 2015a) also observed a size decrease (from 83 to 42 nm) but varying both the organic phase and water temperatures from 20 °C to 60 °C. Their system was composed of MCT/Tween® 80/water with a SOR = 2. As another example, by varying the water temperature from 25 °C to 75 °C with a constant organic phase temperature of 50 °C, An et al. (An et al., 2014) have observed a LNE size decrease from 160 nm at 25 °C to 40 nm at 50 °C; and then an increase to 60 nm at 75 °C. Their system was composed of (capsanthin + MCT)/(Tween® 80 + Span® 20)/water with a SOR = 2.

The phenomenology of these systems is very complex and has been reviewed recently by Komaiko et al. (Komaiko and McClements, 2016). The formation of spontaneous LNEs seems to be governed by a delicate balance between (i) the viscosity of the organic phase (oil + surfactant (s)), (ii) an optimal HLB as discussed in point 3.1, (iii) a low water-oil interfacial tension after the water addition and (iv) the water diffusivity in the organic phase. However, no simple correlation has been determined yet between the LNE size or polydispersity and all these parameters.

Considering our system, as expected, the viscosity of the organic phase decreased with the increase of the temperature (Fig. 6). Its behavior can be fitted with the Frenkel-Andrade model (Frenkel, 1959) which assumes that the viscosity is a thermally activated process (Eq. (5)):

$$\mu(T) = B \cdot exp\left(\frac{E_a}{RT}\right) \quad (5)$$

With B a constant and E_a the activation energy. Linear fits of the experimental data gave an average value close to 35 kJ/mol for Kolliphor + Labrafac mixtures and 25 kJ/mol for pure Labrafac. For classical oils, similar values were obtained in the literature (Giap, 2010).

For this study, no drastic size changes were observed as a function of the organic phase temperature for various SOR from 0.8 to 3. Then, it can be assumed that the viscosity effects favoring good dynamics of the components are balanced with the Kolliphor HLB variation. This HLB is controlled by the number of bound water molecules per ethylene oxide group (Israelachvili, 1997; Picquart et al., 2005) which decreases as the temperature increases.

Concerning the LNE polydispersity, all the formulations were monomodal. Interestingly, reducing the temperature of the organic phase from 90 °C to 30 °C induced a significant reduction of the PDI. At 90 °C, almost all the LNEs had a PDI ranging from 0.15 to 0.20 whereas at 30 °C, almost all the formulas had a PDI lower than 0.15. Reducing the temperature difference between water and the organic phase seemed to favor the formation of a better-controlled nanoemulsion. This work demonstrates that at 30 °C, whatever the targeted size may be (from 20 to 120 nm), there exists an optimized SpKR that ensures a PDI smaller than 0.14 (Fig. 7).

Considering the iso-size and iso-PDI lines, it is possible to define a domain where ternary mixtures made possible the formulation of LNEs from 20 nm to 120 nm with a minimized PDI. This domain corresponds to the blue rectangular area in Fig. 7. In this way, for each targeted size, the Span concentration had to be adjusted so the PDI is optimal, i.e. at least less than 0.14.

3.3. Stability of LNEs at 4 °C and 37 °C

At 4 °C, LNEs were stored without any dilution (stock conditions). As indicated in the materials and methods section, the samples stored at 37 °C were prepared with a 1/400 dilution. The first reason was to mimic biological conditions. The second reason was to investigate the stability of LNEs in a less favorable thermodynamic environment as dilution could decrease their stability. In fact, with this dilution, the Kolliphor concentration was around or below the CMC (60–100 µM (Shubber et al., 2015)), depending on the compositions. For drug delivery purposes, a third reason for testing this dilution was to obtain a Kolliphor concentration below the cytotoxicity threshold (50%-lethal concentration is 3.5 fold the CMC (Le Roux et al., 2017)).

The droplet diameter was used as a stability indicator. As an illustration, Fig. 8 shows the results obtained for the sample n°7, i.e. the central point of the Design Space, repeated four times. The samples produced at the three temperatures were stable after 14 days at 37 °C. Small size modifications were attributed to the statistical errors of the measurement. Therefore, the absence of significant size modification with time was in agreement with the absence of destabilization phenomena that traditionally occur with nanoemulsions, i.e. aggregation, coalescence or Ostwald ripening. This result confirmed the good stability of these LNEs, even in very dilute conditions at 37 °C.

The same interesting stability results were obtained after 30 days of storage conditions of 4 °C with no dilution (Fig. S1 of the Supplementary material).

4. Conclusion

This study confirmed that LNEs with a diameter from 20 nm to 120 nm could be obtained with a low-energy and easy to implement spontaneous self-emulsification. In an eco-design approach and in order to formulate nano-pharmaceutics with thermo-sensitive active molecules, this method could be achieved at three different temperatures for

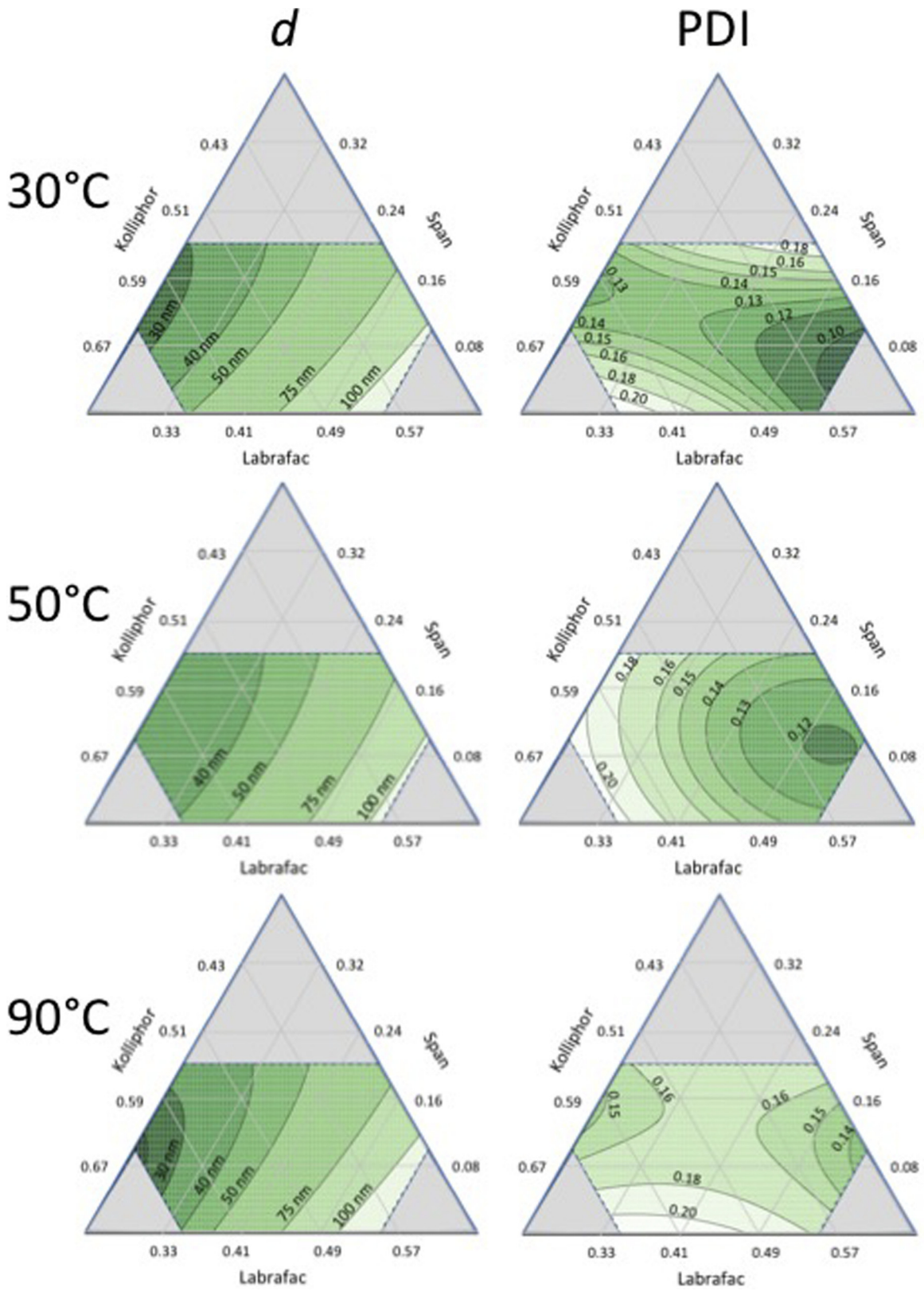

Fig. 4. Results of the mixture experiments on pseudo-ternary diagrams. On the left side, diagrams show the droplet average diameter *d* as a function of the oil/surfactant/cosurfactant composition for the three different temperatures (30 °C, 50 °C and 90 °C). On the right side, diagrams show the polydispersity index (PDI) for the same temperatures and compositions. Lines inside diagrams, with corresponding values, show iso responses (d or PDI).

the organic phase (30 °C, 50 °C and 90 °C) with similar results, water being added at room temperature. LNE sizes were similar for the three temperatures and the PDI was even smaller when the temperature was decreased to 30 °C. The mixture experiment was a suitable tool to obtain a predictive model for LNE size and PDI at every temperature as a function of the organic phase composition, i.e. oil, surfactant and

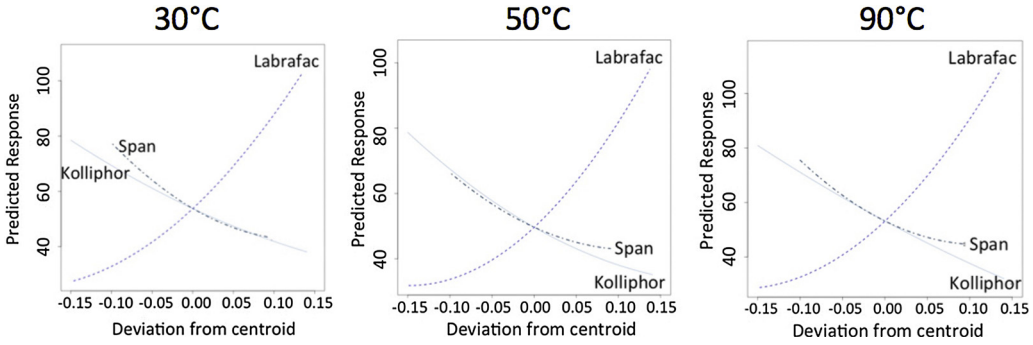

Fig. 5. Effect of Kolliphor, Labrafac and Span concentrations on LNE size (Cox direction).

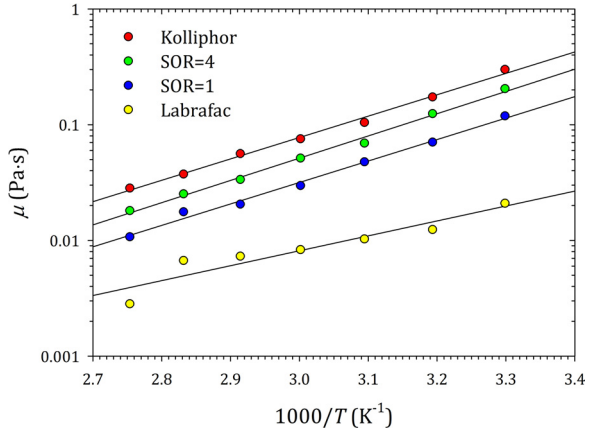

Fig. 6. Evolution of the viscosity of various Labrafac + Kolliphor mixtures as a function of $1/T$. Mixture compositions are indicated in the figure. Straight lines show linear fits to the experimental data (see the text for details).

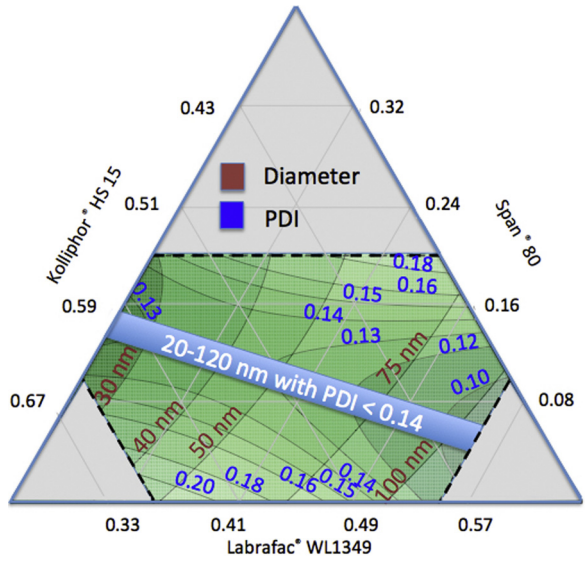

Fig. 7. Combined results of LNE diameters and PDIs obtained for an organic phase temperature of 30 °C. The blue rectangle illustrates the area where the LNEs have the smallest PDIs (< 0.14). (For interpretation of the references to colour in this figure legend, the reader is referred to the web version of this article.)

cosurfactant weight fractions. At 30 °C, the Span (cosurfactant) concentration could be optimized in order to ensure the minimum PDI whatever the targeted droplet diameter may be. Formulated LNEs were stable during at least 30 days at 4 °C in storage conditions and 14 days at 37 °C in dilute conditions in order to target a Kolliphor concentration below its cytotoxicity threshold. This study has confirmed that spontaneous LNEs are easy-to-formulate systems. To improve their

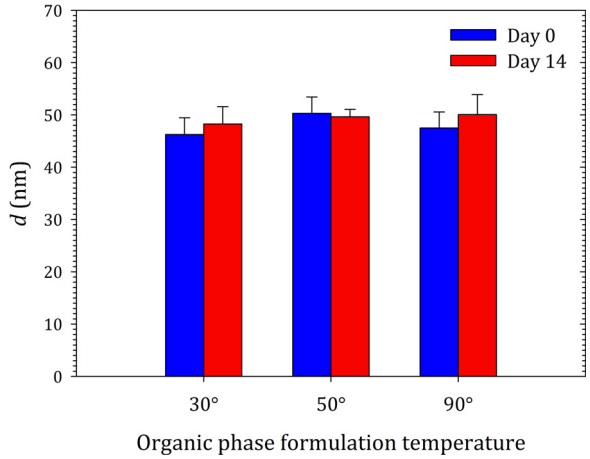

Fig. 8. Stability of LNEs in dilute conditions (1/400) at 37 °C estimated by the droplet diameter evolution between Day 0 (in blue) and Day 14 (in red) at the three tested temperatures for the organic phase (sample n°7 of the Design Space of the mixture experiments, n = 4, mean ± SD). (For interpretation of the references to colour in this figure legend, the reader is referred to the web version of this article.)

potentiality as drug nano-carriers, an increase of the mono-dispersity by a better control of operating parameters, e.g. mixing conditions of organic and aqueous phases, is an interesting direction to pursue the investigation.

Acknowledgements

This work was supported by the MIT-France program from the MIT International Science and Technology Initiatives (MISTI) for the internship of Kristen Frombach. The authors are also grateful for the technical support from Nicolas Rolley for its implication in the preliminary study on screening formulations.

Appendix A. Supplementary data

Supplementary data associated with this article can be found, in the online version, at https://doi.org/10.1016/j.ijpharm.2017.10.017.

References

An, Y., Yan, X., Li, B., Li, Y., 2014. Microencapsulation of capsanthin by self-emulsifying nanoemulsions and stability evaluation. Eur. Food Res. Technol. 239, 1077–1085. http://dx.doi.org/10.1007/s00217-014-2328-3.

Anton, N., Vandamme, T.F., 2009. The universality of low-energy nano-emulsification. Int. J. Pharm. 377, 142–147. http://dx.doi.org/10.1016/j.ijpharm.2009.05.014.

Anton, N., Vandamme, T.F., 2011. Nano-emulsions and micro-emulsions: clarifications of the critical differences. Pharm. Res. 28, 978–985. http://dx.doi.org/10.1007/s11095-010-0309-1.

Anton, N., Gayet, P., Benoit, J.-P., Saulnier, P., 2007. Nano-emulsions and nanocapsules by the PIT method: an investigation on the role of the temperature cycling on the emulsion phase inversion. Int. J. Pharm., New Trends Drug Deliv. Syst. 344, 44–52. http://dx.doi.org/10.1016/j.ijpharm.2007.04.027.

Anton, N., Benoit, J.-P., Saulnier, P., 2008. Design and production of nanoparticles formulated from nano-emulsion templates-a review. J. Controlled Release Off. J. Control. Release Soc. 128, 185–199. http://dx.doi.org/10.1016/j.jconrel.2008.02.007.

Béduneau, A., Hindré, F., Clavreul, A., Leroux, J.-C., Saulnier, P., Benoit, J.-P., 2008. Brain targeting using novel lipid nanovectors. J. Controlled Release 126, 44–49. http://dx.doi.org/10.1016/j.jconrel.2007.11.001.

Berne, B.J., Pecora, R., 2000. Dynamic Light Scattering: With Applications to Chemistry, Biology, and Physics. Dover Publications, Mineola.

Blin, J.-L., Stébé, M.-J., Lebeau, B., 2016. Hybrid/porous materials obtained from nanoemulsions. Curr. Opin. Colloid Interface Sci. 25, 75–82. http://dx.doi.org/10.1016/j.cocis.2016.07.002.

Bouchaala, R., Mercier, L., Andreiuk, B., Mély, Y., Vandamme, T., Anton, N., Goetz, J.G., Klymchenko, A.S., 2016. Integrity of lipid nanocarriers in bloodstream and tumor quantified by near-infrared ratiometric FRET imaging in living mice. J. Control. Release Off. J. Control. Release Soc. 236, 57–67. http://dx.doi.org/10.1016/j.jconrel.2016.06.027.

Bouchemal, K., Briançon, S., Perrier, E., Fessi, H., 2004. Nano-emulsion formulation using spontaneous emulsification: solvent, oil and surfactant optimisation. Int. J. Pharm. 280, 241–251. http://dx.doi.org/10.1016/j.ijpharm.2004.05.016.

Calligaris, S., Plazzotta, S., Bot, F., Grasselli, S., Malchiodi, A., Anese, M., 2016. Nanoemulsion preparation by combining high pressure homogenization and high power ultrasound at low energy densities. Food Res. Int. 83, 25–30. http://dx.doi.org/10.1016/j.foodres.2016.01.033.

Cox, D.R., 1971. A note on polynomial response functions for mixtures. Biometrika 58, 155–159. http://dx.doi.org/10.2307/2334326.

Dai, L., Li, W., Hou, X., 1997. Effect of the molecular structure of mixed nonionic surfactants on the temperature of miniemulsion formation. Colloids Surf. Physicochem. Eng. Asp. 125, 27–32. http://dx.doi.org/10.1016/S0927-7757(96)03859-9.

Date, A.A., Nagarsenker, M.S., 2007. Design and evaluation of self-nanoemulsifying drug delivery systems (SNEDDS) for cefpodoxime proxetil. Int. J. Pharm. 329, 166–172. http://dx.doi.org/10.1016/j.ijpharm.2006.08.038.

Date, A.A., Desai, N., Dixit, R., Nagarsenker, M., 2010. Self-nanoemulsifying drug delivery systems: formulation insights, applications and advances. Nanomed 5, 1595–1616. http://dx.doi.org/10.2217/nnm.10.126.

Davidov-Pardo, G., McClements, D.J., 2015. Nutraceutical delivery systems: resveratrol encapsulation in grape seed oil nanoemulsions formed by spontaneous emulsification. Food Chem. 167, 205–212. http://dx.doi.org/10.1016/j.foodchem.2014.06.082.

Dixit, R.P., Nagarsenker, M.S., 2008. Self-nanoemulsifying granules of ezetimibe: design, optimization and evaluation. Eur. J. Pharm. Sci. 35, 183–192. http://dx.doi.org/10.1016/j.ejps.2008.06.013.

Forgiarini, A., Esquena, J., González, C., Solans, C., 2000. Studies of the relation between phase behavior and emulsification methods with nanoemulsion formation. Prog. Colloid Polym. Sci. 115, 36–39.

Forgiarini, A., Esquena, J., González, C., Solans, C., 2001. Formation of nano-emulsions by low-Energy emulsification methods at constant temperature. Langmuir 17, 2076–2083. http://dx.doi.org/10.1021/la001362n.

Frenkel, Y.I., 1959. Kinetic Theory of Liquids. Izd. Akad. Nauk SSSR, Moscow–Leningrad.

Giap, S.G.E., 2010. The hidden property of Arrhenius-type relationship: viscosity as a function of temperature. J. Phys. Sci. 21, 29–39.

Goindi, S., Kaur, A., Kaur, R., Kalra, A., Chauhan, P., 2016. 19 − nanoemulsions: an emerging technology in the food industry A2 − grumezescu, alexandru mihai. Emulsions. Academic Press, pp. 651–688. http://dx.doi.org/10.1016/B978-0-12-804306-6.00019-2.

Gutiérrez, J.M., González, C., Maestro, A., Solè, I., Pey, C.M., Nolla, J., 2008. Nano-emulsions: new applications and optimization of their preparation. Curr. Opin. Colloid Interface Sci. 13, 245–251. http://dx.doi.org/10.1016/j.cocis.2008.01.005.

Hörmann, K., Zimmer, A., 2016. Drug delivery and drug targeting with parenteral lipid nanoemulsions — A review. J. Controlled Release 223, 85–98. http://dx.doi.org/10.1016/j.jconrel.2015.12.016.

Heurtault, B., Saulnier, P., Benoit, J.-P., Proust, J.-E., Pech, B., Richard, J., 2001. Nanocapsules lipidiques. Procede De Preparation Et Utilisation Comme Medicament (WO/2001/064328).

Heurtault, B., Saulnier, P., Pech, B., Venier-Julienne, M.-C., Proust, J.-E., Phan-Tan-Luu, R., Benoît, J.-P., 2003. The influence of lipid nanocapsule composition on their size distribution. Eur. J. Pharm. Sci. 18, 55–61. http://dx.doi.org/10.1016/S0928-0987(02)00241-5.

Huynh, N.T., Passirani, C., Saulnier, P., Benoit, J.P., 2009. Lipid nanocapsules: a new platform for nanomedicine. Int. J. Pharm. Challenges Nanotechnol. Delivery Imaging 379, 201–209. http://dx.doi.org/10.1016/j.ijpharm.2009.04.026.

Israelachvili, J., 1997. The different faces of poly(ethylene glycol). Proc. Natl. Acad. Sci. U. S. A. 94, 8378–8379.

Israelachvili, J.N., 2011. Intermolecular and Surface Forces, 3rd ed. Academic Press, Burlington, MA.

Izquierdo, P., Esquena, J., Tadros, T.F., Dederen, J.C., Feng, J., Garcia-Celma, M.J., Azemar, N., Solans, C., 2004. Phase behavior and nano-emulsion formation by the phase inversion temperature method. Langmuir ACS J. Surf. Colloids 20, 6594–6598. http://dx.doi.org/10.1021/la049566h.

Khani, S., Keyhanfar, F., Amani, A., 2016. Design and evaluation of oral nanoemulsion drug delivery system of mebudipine. Drug Deliv. 23, 2035–2043. http://dx.doi.org/10.3109/10717544.2015.1088597.

Komaiko, J., McClements, D.J., 2015a. Food-grade nanoemulsion filled hydrogels formed by spontaneous emulsification and gelation: optical properties, rheology, and stability. Food Hydrocoll. 46, 67–75. http://dx.doi.org/10.1016/j.foodhyd.2014.12.031.

Komaiko, J., McClements, D.J., 2015b. Low-energy formation of edible nanoemulsions by spontaneous emulsification: factors influencing particle size. J. Food Eng. 146, 122–128. http://dx.doi.org/10.1016/j.jfoodeng.2014.09.003.

Komaiko, J.S., McClements, D.J., 2016. Formation of food-Grade nanoemulsions using low-Energy preparation methods: a review of available methods. Compr. Rev. Food Sci. Food Saf. 15, 331–352. http://dx.doi.org/10.1111/1541-4337.12189.

Kuhn, K.R., Cunha, R.L., 2012. Flaxseed oil −Whey protein isolate emulsions: effect of high pressure homogenization. J. Food Eng. 111, 449–457. http://dx.doi.org/10.1016/j.jfoodeng.2012.01.016.

Lawson, J., Willden, C., 2016. Mixture experiments in r using mixexp. J. Stat. Softw. 72, 1–20.

Le Roux, G., Moche, H., Nieto, A., Benoit, J.-P., Nesslany, F., Lagarce, F., 2017. Cytotoxicity and genotoxicity of lipid nanocapsules. Toxicol. In Vitro 41, 189–199. http://dx.doi.org/10.1016/j.tiv.2017.03.007.

Lin, T.J., Kurihara, H., Ohta, H., 1975. Effects of phase inversion and surfactant location on the formation of O/W emulsions. J. Soc. Cosmet. Chem. 26, 121–139.

Liu, W., Sun, D., Li, C., Liu, Q., Xu, J., 2006. Formation and stability of paraffin oil-in-water nano-emulsions prepared by the emulsion inversion point method. J. Colloid Interface Sci. 303, 557–563. http://dx.doi.org/10.1016/j.jcis.2006.07.055.

Matougui, N., Boge, L., Groo, A.-C., Umerska, A., Ringstad, L., Bysell, H., Saulnier, P., 2016. Lipid-based nanoformulations for peptide delivery. Int. J. Pharm. 502, 80–97. http://dx.doi.org/10.1016/j.ijpharm.2016.02.019.

McClements, D.J., 2011. Edible nanoemulsions: fabrication, properties, and functional performance. Soft Matter 7, 2297–2316. http://dx.doi.org/10.1039/C0SM00549E.

McClements, D.J., 2012. Nanoemulsions versus microemulsions: terminology, differences, and similarities. Soft Matter 8, 1719. http://dx.doi.org/10.1039/c2sm06903b.

Mishra, R.K., Soni, G.C., Mishra, R., 2015. Nanoemulsion: a novel drug delivery tool. Int. J. Pharma Res. Rev. 2014.

Montenegro, L., Lai, F., Offerta, A., Sarpietro, M.G., Micicchè, L., Maccioni, A.M., Valenti, D., Fadda, A.M., 2016. From nanoemulsions to nanostructured lipid carriers: a relevant development in dermal delivery of drugs and cosmetics. J. Drug Deliv. Sci. Technol., Drug Delivery Research in Italy 32 100–112. http://dx.doi.org/10.1016/j.jddst.2015.10.003.

Pchelintsev, N.A., Adams, P.D., Nelson, D.M., 2016. Critical parameters for efficient sonication and improved chromatin immunoprecipitation of high molecular weight proteins. PLoS One 11. http://dx.doi.org/10.1371/journal.pone.0148023.

Picquart, M., Valdez, D., Vázquez, H., Urbach, W., Waks, M., Hernández-Pozos, J.L., Olayo-Gonzalez, R., 2005. Bound and free water In surfactant micelles and lipid vesicles. AIP Conf. Proc. 759, 103–110. http://dx.doi.org/10.1063/1.1928163.

Pouton, C.W., 1997. Formulation of self-emulsifying drug delivery systems. the potential of oily formulations for drug delivery to the gastro-intestinal tract. Adv. Drug Deliv. Rev. 25, 47–58. http://dx.doi.org/10.1016/S0169-409X(96)00490-5.

R Development Core Team, 2014. R: A Language and Environment for Statistical Computing. R Foundation for Statistical Computing, Vienna, Austria.

Roger, E., Lagarce, F., Benoit, J.-P., 2009. The gastrointestinal stability of lipid nanocapsules. Int. J. Pharm. Challenges for Nanotechnol. Delivery Imaging 379, 260–265. http://dx.doi.org/10.1016/j.ijpharm.2009.05.069.

Saberi, A.H., Fang, Y., McClements, D.J., 2013. Fabrication of vitamin E-enriched nanoemulsions: factors affecting particle size using spontaneous emulsification. J. Colloid Interface Sci. 391, 95–102. http://dx.doi.org/10.1016/j.jcis.2012.08.069.

Sagitani, H., 1981. Making homogeneous and fine droplet O/W emulsions using nonionic surfactants. J. Am. Oil Chem. Soc. 58, 738–743. http://dx.doi.org/10.1007/BF02899466.

Shen, J., Bi, J., Tian, H., Jin, Y., Wang, Y., Yang, X., Yang, Z., Kou, J., Li, F., 2016. Preparation and evaluation of a self-nanoemulsifying drug delivery system loaded with Akebia saponin D?phospholipid complex. Int. J. Nanomed. 11, 4919–4929. http://dx.doi.org/10.2147/IJN.S108765.

Shinoda, K., Saito, H., 1968. The effect of temperature on the phase equilibria and the types of dispersions of the ternary system composed of water, cyclohexane, and nonionic surfactant. J. Colloid Interface Sci. 26, 70–74. http://dx.doi.org/10.1016/0021-9797(68)90273-7.

Shinoda, K., Saito, H., 1969. The Stability of O/W type emulsions as functions of temperature and the HLB of emulsifiers: the emulsification by PIT-method. J. Colloid Interface Sci. 30, 258–263. http://dx.doi.org/10.1016/S0021-9797(69)80012-3.

Shubber, S., Vllasaliu, D., Rauch, C., Jordan, F., Illum, L., Stolnik, S., 2015. Mechanism of mucosal permeability enhancement of CriticalSorb® (Solutol® HS15) investigated in vitro in cell cultures. Pharm. Res. 32, 516–527. http://dx.doi.org/10.1007/s11095-014-1481-5.

Singh, Y., Meher, J.G., Raval, K., Khan, F.A., Chaurasia, M., Jain, N.K., Chourasia, M.K., 2017. Nanoemulsion: concepts, development and applications in drug delivery. J. Controlled Release 252, 28–49. http://dx.doi.org/10.1016/j.jconrel.2017.03.008.

Solans, C., Solé, I., 2012. Nano-emulsions: formation by low-energy methods. Curr. Opin. Colloid Interface Sci. 17, 246–254. http://dx.doi.org/10.1016/j.cocis.2012.07.003.

Solans, C., Izquierdo, P., Nolla, J., Azemar, N., Garcia-Celma, M.J., 2005. Nano-emulsions. Curr. Opin. Colloid Interface Sci. 10, 102–110. http://dx.doi.org/10.1016/j.cocis.2005.06.004.

Trotta, M., Gallarate, M., Pattarino, F., Morel, S., 2001. Emulsions containing partially water-miscible solvents for the preparation of drug nanosuspensions. J. Control. Release Off J. Control. Release Soc. 76, 119–128.

Yoo, J.H., Shanmugam, S., Thapa, P., Lee, E.-S., Balakrishnan, P., Baskaran, R., Yoon, S.-K., Choi, H.-G., Yong, C.S., Yoo, B.K., Han, K., 2010. Novel self-nanoemulsifying drug delivery system for enhanced solubility and dissolution of lutein. Arch. Pharm. Res. 33, 417–426.

Yukuyama, M.N., Ghisleni, D.D.M., Pinto, T.J.A., Bou-Chacra, N.A., 2016. Nanoemulsion: process selection and application in cosmetics–a review. Int. J. Cosmet. Sci. 38, 13–24. http://dx.doi.org/10.1111/ics.12260.

Zeng, L., Zhang, Y., 2016. Impact of short-chain alcohols on the formation and stability of nano-emulsions prepared by the spontaneous emulsification method. Colloids Surf. Physicochem. Eng. Asp. 509, 591–600. http://dx.doi.org/10.1016/j.colsurfa.2016.09.001.

Zhang, H., Wang, Z., Liu, O., 2016. Simultaneous determination of kolliphor HS15 and miglyol 812 in microemulsion formulation by ultra-high performance liquid chromatography coupled with nano quantity analyte detector. J. Pharm. Anal. 6, 11–17. http://dx.doi.org/10.1016/j.jpha.2015.11.004.

Zhao, L., Wei, Y., Huang, Y., He, B., Zhou, Y., Fu, J., 2013. Nanoemulsion improves the oral bioavailability of baicalin in rats: in vitro and in vivo evaluation. Int. J. Nanomed. 8, 3769–3779. http://dx.doi.org/10.2147/IJN.S51578.